

# REPORT DOCUMENTATION PAGE

Form Approved  
OMB NO. 0704-0188

Public Reporting burden for this collection of information is estimated to average 1 hour per response, including the time for reviewing instructions, searching existing data sources, gathering and maintaining the data needed, and completing and reviewing the collection of information. Send comment regarding this burden estimates or any other aspect of this collection of information, including suggestions for reducing this burden, to Washington Headquarters Services, Directorate for information Operations and Reports, 1215 Jefferson Davis Highway, Suite 1204, Arlington, VA 22202-4302, and to the Office of Management and Budget, Paperwork Reduction Project (0704-0188,) Washington, DC 20503.

1. AGENCY USE ONLY (Leave Blank)

2. REPORT DATE  
November 30<sup>th</sup>, 2005

3. REPORT TYPE AND DATES COVERED

Final progress report  
01 May 02 - 30 Aug 05

4. TITLE AND SUBTITLE

Biocatalytic Buffering System for Detoxification of Nerve Agents

5. FUNDING NUMBERS

DAAD19-02-1-0072

6. AUTHOR(S)

Joel L. Kaar, Richard Koepsel, Alan J. Russell

7. PERFORMING ORGANIZATION NAME(S) AND ADDRESS(ES)

University of Pittsburgh  
100 Technology Drive, Suite #200  
Pittsburgh, PA 15218

8. PERFORMING ORGANIZATION  
REPORT NUMBER

9. SPONSORING / MONITORING AGENCY NAME(S) AND ADDRESS(ES)

U. S. Army Research Office  
P.O. Box 12211  
Research Triangle Park, NC 27709-2211

10. SPONSORING / MONITORING  
AGENCY REPORT NUMBER

42617.1-CH

11. SUPPLEMENTARY NOTES

The views, opinions and/or findings contained in this report are those of the author(s) and should not be construed as an official Department of the Army position, policy or decision, unless so designated by other documentation.

12 a. DISTRIBUTION / AVAILABILITY STATEMENT

Approved for public release; distribution unlimited.

12 b. DISTRIBUTION CODE

13. ABSTRACT (Maximum 200 words)

A major obstacle in the utility of enzymes for decontamination purposes is their sensitivity to their surrounding environment. Enzymes are only catalytically active within a narrow range of conditions including pH and temperature. Sensitivity to pH is of particular importance in hydrolysis reactions due to the generation of acidic products. In the enzymatic hydrolysis of nerve agents, to prevent inactivation of the enzyme prior to complete conversion of the toxin, tight control of pH over the full time course of detoxification is required. To counter this sensitivity, we have developed a method of controlling pH during enzyme-mediated detoxification by using the urease-catalyzed hydrolysis of urea. Base generated by urea hydrolysis neutralizes the formation of acid such that a dynamic pH equilibrium is created between the competing reactions. We have successfully demonstrated the use of biocatalytic pH control in the detoxification of both paraoxon and DFP by OPH. Results indicated that urease from jack bean and *Helicobacter pylori* were significantly inhibited by fluoride, a product DFP hydrolysis, at concentrations in the micromolar range. Means of overcoming this inhibition including the use of fluoride scavengers and alternative base-producing enzymatic reactions was studied.

**ARO FINAL REPORT**

**Project Title: Biocatalytic Buffering System for Detoxification of Nerve Agents**

**Proposal Number: 42617-CH**

**Agreement Number: DAAD19-02-1-0072**

Joel L. Kaar, Richard Koepsel, and Alan J. Russell\*

*McGowan Institute for Regenerative Medicine, Suite 200, 100 Technology Drive,  
University of Pittsburgh, Pittsburgh, Pennsylvania 15219*

\*Principal investigator:

Dr. Alan J. Russell

Email: russellaj@msx.upmc.edu

Tel: (412) 235-5109

Fax: (412) 235-5290

## TABLE OF CONTENTS

<b>Statement of Problem Studied</b> .....	1
<b>Summary of Results</b> .....	3
<i>Modeling of dynamic pH equilibrium</i> .....	3
<i>Impact of fluoride on urease buffering</i> .....	9
<i>Improving resistance of biocatalytic buffers to fluoride inhibition</i> .....	12
<i>Biocatalytic pH control in low-water environments</i> .....	17
<b>Conclusions</b> .....	20
<b>Summary of Papers Published or Presented</b> .....	21
<b>Technical Reports Submitted to ARO</b> .....	21
<b>Scientific Personnel Supported by the Project</b> .....	22

## **Statement of Problem Studied**

A major limitation in the enzymatic detoxification of nerve agents is the generation of large quantities of acid, which has a significant adverse impact on biocatalyst efficiency. To prevent inactivation of the enzyme prior to complete conversion of the toxin, tight control of pH over the full time course of detoxification is required.

Currently, the preferred buffer for enzymatic decontamination systems under development by the U.S. Army is ammonium carbonate. The addition of solid ammonium carbonate to water results in a pH of 8.5 to 9.0 with no adjustment needed, and the ammonium ions are known to stimulate the activity of OPAA. Ammonium carbonate and other conventional biological buffers, however, have low buffering capacities, thus making them impractical for use in large scale decontamination.

The buffering requirement is amplified in water restricted environments, where the solubility of nerve agents is increased. Based on the chemical agent challenge specified by the North Atlantic Treaty Organization (10 g of agent per m<sup>2</sup>), the concentration of agent in detergent and microemulsion systems, which typically consist of 1 to 10 vol % aqueous phase, can exceed 0.5 M in 1L of decontaminant. To buffer complete decontamination, conventional buffers such as HEPES would be required at concentrations greater than 28 % (w/v) resulting in solubility problems (e.g. the solubility limit of HEPES is 26%). Additional problems associated with the use of conventional buffers at concentrations sufficient to maintain pH in an optimum range for enzyme activity in such systems include enzyme inhibition and chelation of catalytically essential metal ions.

Biocatalytic buffering is a unique alternative method to pH control in which the hydrolytic activity of an acid-producing enzyme is coupled with the enzymatic generation of base. In an unbuffered solution, the formation of acid by enzymatic hydrolysis of a nerve agent causes a rapid drop in pH. As a result, the pH ultimately reaches a point at which the enzyme is completely inactivated.

By supplementing the same solution with a second enzyme that catalyzes the formation of base, the acidic products resulting from nerve agent hydrolysis can be neutralized. In this system, the base-producing enzyme has a pH optimum significantly lower than that of the acid-producing enzyme (**Figure 1**). The formation of base counteracts the production of acid, thereby creating a dynamic pH equilibrium between the competing reactions. Because the generation of base is biocatalytic, base is produced only in response to a decrease in pH. The position of the pH equilibrium in theory remains unchanged as long as the activities of the enzymes remain constant. Furthermore, by altering the ratio of activities of the enzymes, the equilibrium position can be controlled.

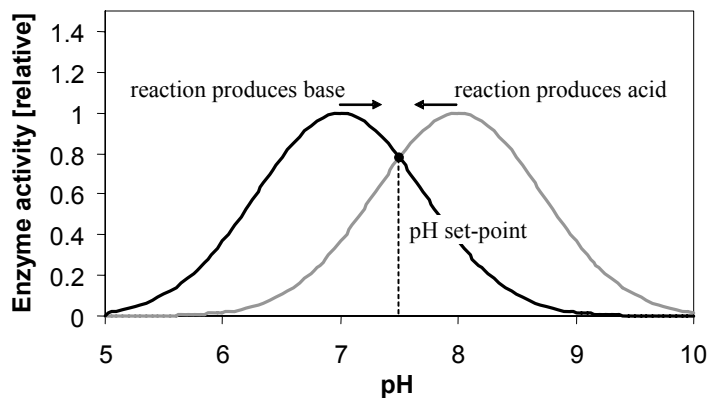


**Figure 1.** The pH dependence curves of two enzyme catalyzed reactions. The base-producing enzyme (black line) has a lower optimal pH than the acid-producing enzyme (gray line). When both enzymes are present, the pH should stabilize at the intersection point, which is termed the pH “set-point”.

Urease-catalyzed urea hydrolysis is an ideal agent for buffering nerve agent degradation. Urea is highly soluble and environmentally safe. The molecular weight of urea is also considerably less than that of conventional buffers. Therefore, substantially less urea is required to neutralize a given amount of acid. This is of particular importance when considering the logistical burden associated with the transportation of detoxification materials. Hydrolysis of urea yields two ammonia molecules and a single molecule of carbonic acid. At near neutral pH, carbonic acid dissociates into bicarbonate, thereby releasing a proton, and the ammonia molecules are protonated, ultimately resulting in a net increase in pH.

## Summary of Results

### *Modeling of dynamic pH equilibrium*

The concept of biocatalytic pH control was initially tested using urease-catalyzed urea hydrolysis to buffer the degradation of paraoxon by OPH. Hydrolysis of paraoxon yields *p*-nitrophenol and diethylphosphoric acid. At neutral pH, both hydrolysis products dissociate into their conjugate base form, resulting in the accumulation of protons. When the hydrolysis of urea and paraoxon occur simultaneously, one would predict that the protons generated during the degradation of paraoxon will be neutralized by hydroxide ions released as a result of urea degradation (**Figure 2**).

(A)

(B)

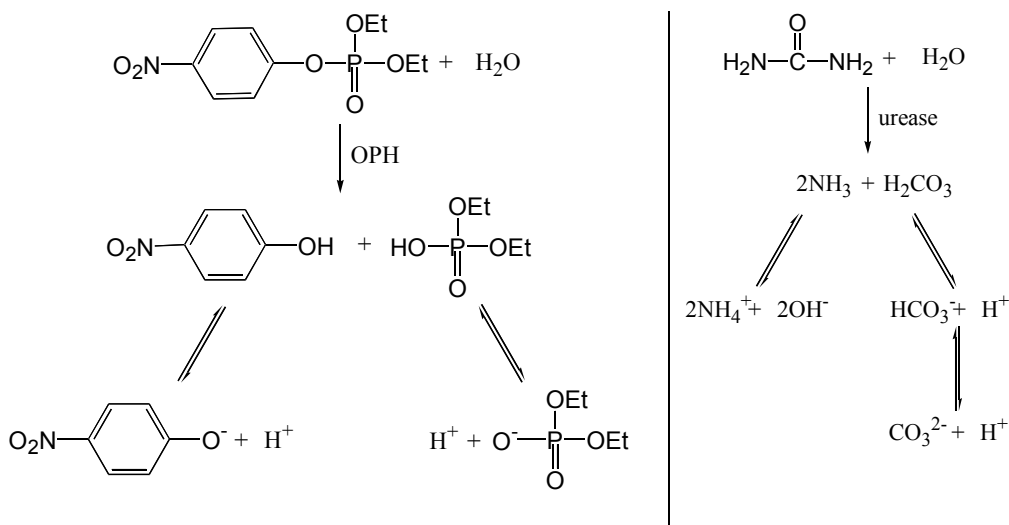


**Figure 2. (A) OPH-catalyzed hydrolysis of paraoxon and (B) urease-catalyzed hydrolysis of urea.**

The pH in the combined enzyme system can be described as a function of time by a proton concentration balance (**Equation 1**). In this equation,  $V_{H^+}$  and  $V_{OH^-}$  represents the rate of formation of acid and base respectively. The net accumulation of protons in the system can also be expressed as the rate of change in pH (**Equation 2**).

$$\frac{d[H^+]}{dt} = V_{H^+} - V_{OH^-} \quad \text{Equation 1}$$

$$\frac{dpH}{dt} = \frac{1}{(-\ln(10))(10^{-pH})} \left( \frac{d[H^+]}{dt} \right) = \frac{1}{(-\ln(10))(10^{-pH})} (V_{H^+} - V_{OH^-}) \quad \text{Equation 2}$$

The rates at which protons and hydroxide ions are generated in this system are dependent upon the rates of paraoxon and urea hydrolysis and the dissociation constants of the respective hydrolysis products. The dissociation of *p*-nitrophenol (pKa, PNP) and diethylphosphoric acid (pKa, DPA) during paraoxon hydrolysis varies with pH and is described by the proportionality factor  $P_{H^+}$  (**Equation 3**). Similarly, the proportionality factor  $P_{OH^-}$  relates the overall release of hydroxide during urea hydrolysis to the

dissociation of ammonia and carbonic acid, which is in equilibrium with bicarbonate and carbonate, as a function of pH (**Equation 4**).

$$P_{H^+} = \frac{1}{1 + 10^{(pKa, PNP - pH)}} + \frac{1}{1 + 10^{(pKa, DPA - pH)}} \quad \text{Equation 3}$$

$$P_{OH^-} = \frac{2}{1 + \frac{K_a, NH_4^+}{10^{-pH}}} - \left[ \frac{1}{1 + 10^{pKa, H_2CO_3 - pH}} - \left( \frac{10^{pH - pKa, HCO_3^-}}{1 + 10^{pKa, H_2CO_3 - pH}} \right) \left( \frac{1}{1 + 10^{pH - pKa, HCO_3^-}} \right) \right] \quad \text{Equation 4}$$

$$- 2 \left[ \left( \frac{10^{pH - pKa, HCO_3^-}}{1 + 10^{pKa, H_2CO_3 - pH}} \right) \left( \frac{1}{1 + 10^{pH - pKa, HCO_3^-}} \right) \right]$$

By substituting the activity of OPH ( $V_{OPH}$ ) and urease ( $V_{urease}$ ) and the proportionality factors into the proton balance, one obtains:

$$\frac{dpH}{dt} = \frac{1}{(-\ln(10))(10^{-pH})} (P_{H^+} V_{OPH} - P_{OH^-} V_{urease}) \quad \text{Equation 5}$$

The activity of OPH is defined using the Michaelis-Menton rate equation (**Equation 6**). Because urease is always saturated with urea in this system, its activity is constant throughout the buffering process. By solving **Equations 5** and **6** simultaneously, the pH and conversion of paraoxon over the time course of the detoxification reaction can be simulated.

$$V_{OPH} = \frac{-d[\text{paraoxon}]}{dt} = \frac{k_{cat} [OPH][\text{paraoxon}]}{K_M + [\text{paraoxon}]} \quad \text{Equation 6}$$

The pH dependence of urease activity was measured in the presence of urea (10 mM) over the pH range 6.5 to 8.2 (**Figure 3A**). The pH-dependence of the kinetic parameters ( $k_{\text{cat}}$  and  $K_M$ ) for OPH-catalyzed degradation of paraoxon were also determined (**Figure 3B**). Because the pH optimum of urease is lower than that of OPH, the enzymes fit the general model depicted in **Figure 2**.

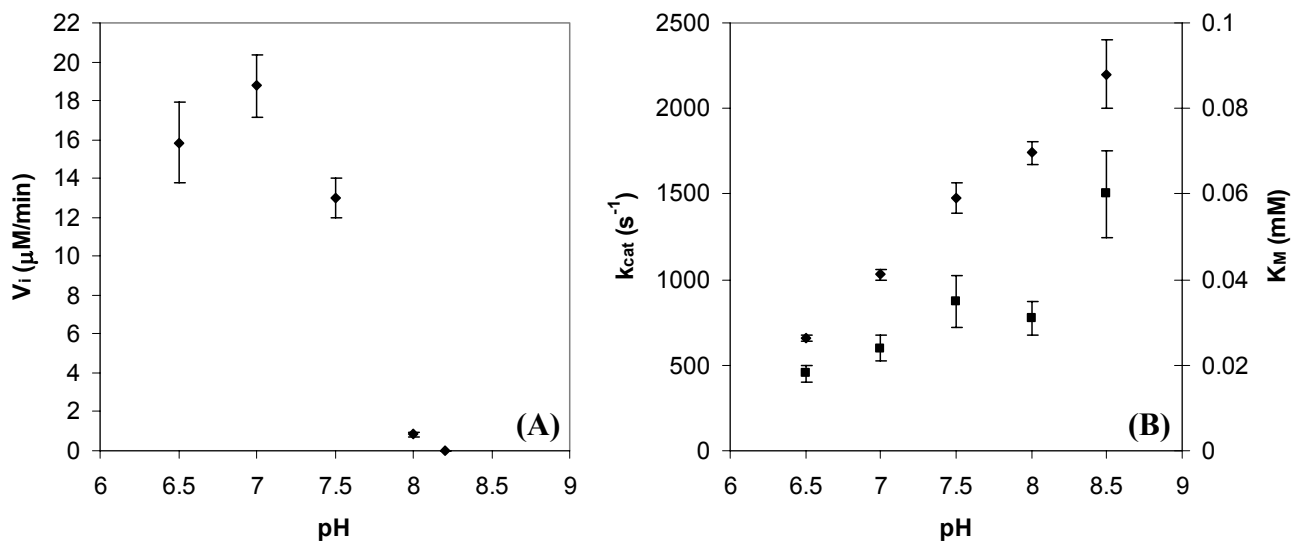


**Figure 3. pH dependence of (A) urease activity and (B) the kinetic parameters ( $k_{\text{cat}}$  (◆) and  $K_M$  (■) for OPH-catalyzed hydrolysis of paraoxon.**

When using a molar ratio of urease to OPH activity of 31, the pH of the system equilibrates at 8.1 within minutes (**Figure 4A**). The predicted pH set-point and paraoxon conversion profile generated by the model closely match the measured values. If the pH of the system were significantly different than the predicted profile, the conversion would likely also deviate from its predicted course. In the absence of urease, the system pH initially decreases rapidly causing the conversion of paraoxon to cease.

The complete degradation of paraoxon was achieved using the same ratio of urease to OPH activity with the respective concentrations increased 6-fold (**Figure 4B**).

As the conversion of paraoxon exceeds 60 %, the pH increases gradually to 8.4, at which point all of the paraoxon is degraded and the activity of urease is negligible. The apparent increase in pH is caused by a decrease of OPH activity. When OPH is no longer saturated with paraoxon, its activity is dependent upon substrate concentration. Therefore, as the conversion of paraoxon approaches 100 %, the rate at which OPH catalyzed the degradation of paraoxon decelerates. Product inhibition, which is not accounted for in the predictive model, may also play a role in reducing the activity of OPH.

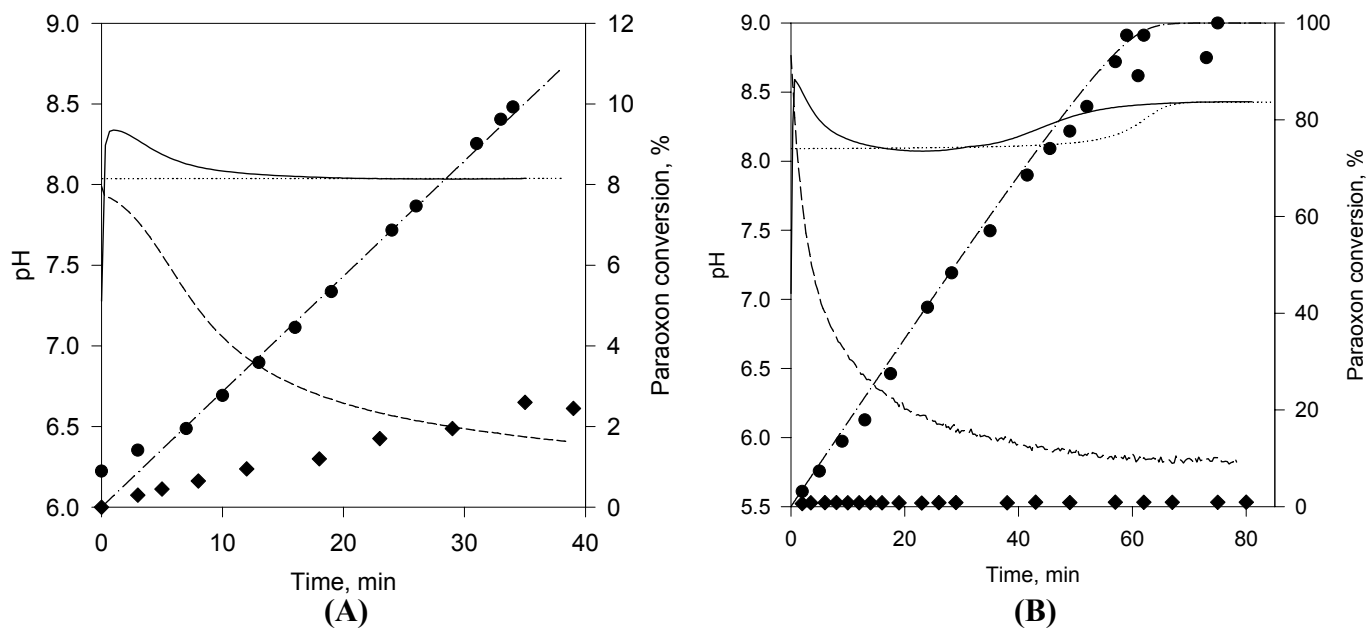


**Figure 4. Degradation of paraoxon buffered by urease-catalyzed hydrolysis of urea. The solid and closed circles represent the measured pH and paraoxon conversion profile respectively in the presence of urease and urea. The dotted and dash-dotted lines correspond to the model predicted pH and paraoxon conversion profile also in the presence of urease and urea. The dashed line and closed diamonds refer to the measured pH and paraoxon conversion profile in the absence of urease. The pH set-point remains constant as long as the ratio of activity of the enzymes is unchanged (A)  $[\text{urease}] = 0.081 \text{ units/mL}$  and  $[\text{OPH}] = 0.0026 \text{ units/mL}$  ( $[\text{urease}]/[\text{OPH}] = 31$ ) (B)  $[\text{urease}] = 0.49 \text{ units/mL}$  and  $[\text{OPH}] = 0.016 \text{ units/mL}$  ( $[\text{urease}]/[\text{OPH}] = 31$ ).**

A similar experiment was performed using a ratio of urease and OPH activities of 0.54 (**Figure 5**). Due to the greater relative concentration of OPH than in the previous experiment, the pH of the system should presumably equilibrate at a lower set-point. As expected, in this system, a pH set-point of 7.2 was experimentally obtained and predicted. It should be noted that initiating the reaction over one pH unit away from the set-point did not affect the equilibration of the system. Additional experiments demonstrated that by altering the ratio of enzyme activities, the pH set-point is controllable between 6.5 and 8.5 (**Figure 6**).

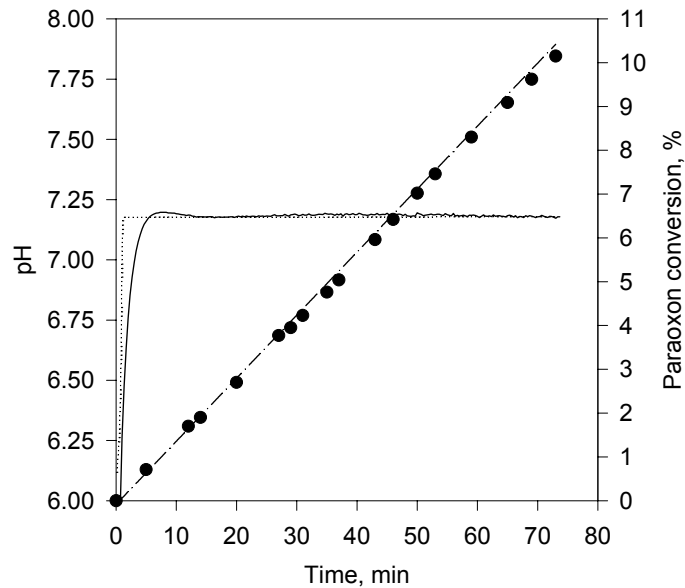


**Figure 5. Buffering of paraoxon degradation using a ratio of urease (0.0025 units/mL) to OPH (0.0047 units/mL) of 0.54.**

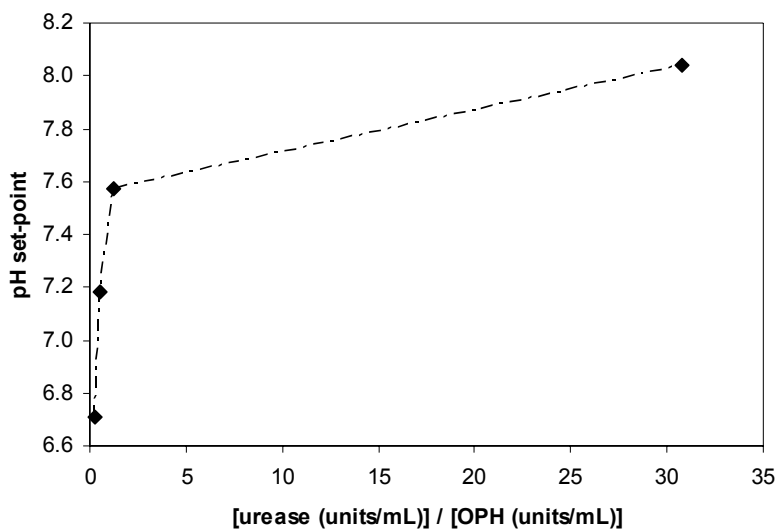


**Figure 6. The impact of the ratio of urease activity to OPH activity on the pH set-point during paraoxon degradation.**

#### *Impact of fluoride on urease buffering*

As one might expect, the inhibition of one or more of the enzymes in biocatalytic buffering systems will alter the pH equilibrium created by the competing reactions. The extent to which the equilibrium position is shifted and the ability to maintain that equilibrium over the full time course of the decontamination reaction is dependent upon the magnitude of the inhibition. Fluoride generated by the degradation of nerve agents that contain a hydrolysable phosphorous-fluorine bond such as sarin, soman, and DFP inhibits ureases and thus presents the potential to destroy the buffering capacity of the previously described OPH-urease system. The key question to be addressed is whether this inhibition prevents the complete conversion of the toxin.

The extent to which jack bean urease is inhibited by fluoride was initially investigated via progress curve analysis in which the formation of ammonia was monitored. In the absence of fluoride, the rate of ammonia production was constant (**Figure 7A**). The initial burst ( $v_0$ ) of urease activity was not affected by the presence of

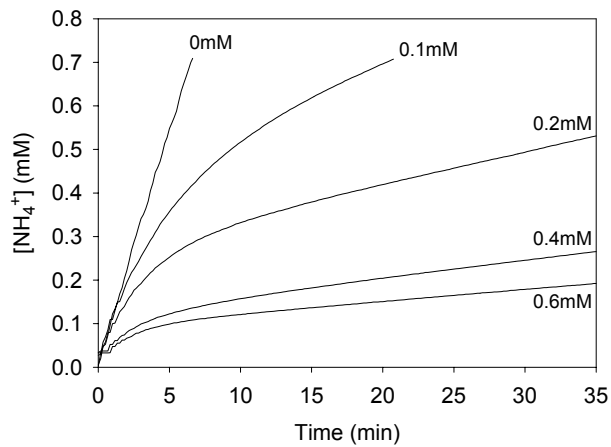
fluoride. However, with fluoride present, the rate at which ammonia was liberated steadily decreased ultimately reaching a final steady-state rate ( $v_f$ ).

Although fluoride concentration had no impact on  $v_o$ ,  $v_f$  and the rate at which  $v_o$  reached  $v_f$  were significantly effected by fluoride level in the enzyme reaction. An increase in fluoride concentration corresponded to a decrease in  $v_f$ . The rate at which  $v_f$  was obtained significantly increased at greater fluoride levels. Todd and Hausinger (*Biochemistry* 2000, 39) reported similar kinetic data in describing the fluoride inhibition of *Klebsiella aerogenes* urease. It was proposed that the mechanism of inhibition involves binding of fluoride to the nickel molecules situated within the enzyme's active site.

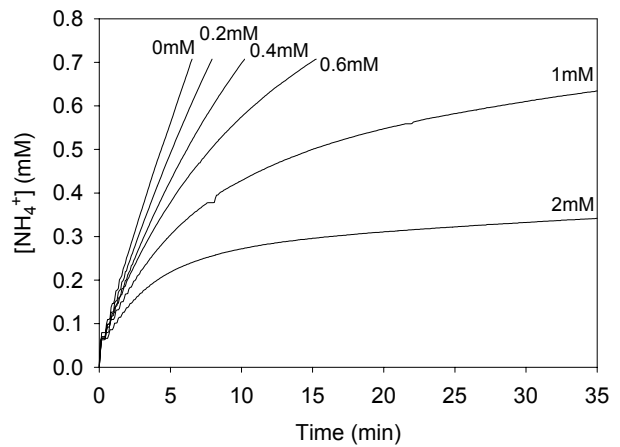
In an attempt to identify fluoride resistant ureases, the sensitivity of several ureases including *Helicobacter pylori* urease, a thermally stable industrial urease from jack bean, and a recombinant *Klebsiella aerogenes* (FRKAU 9-1) mutant urease to fluoride was screened. The *H. pylori* urease was expressed from a bacterial culture supplied by Dr. Harry L.T. Mobley from the University of Maryland School of Medicine. The industrial urease was obtained as a gift from Roche Diagnostics. FRKAU 9-1 mutant urease was provided by Dr. Joseph J. DeFrank from the US Army Edgewood Chemical and Biological Center (ECBC). The mutant enzyme was isolated after successive rounds of growth in fluoride-containing culture media.

Results of the screening indicated that all three of the ureases were in fact inhibited by fluoride in a time-dependent manner similar to that observed in the inhibition of jack bean urease (**Figure 7B-D**). Of all the enzymes screened, *H. pylori* urease appeared to be the most fluoride resistant. Nonetheless, with just 2 mM fluoride present,

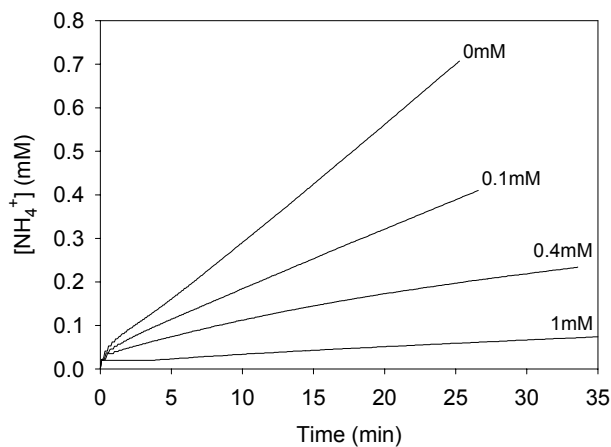
*H. pylori* urease lost greater than 98 % of its initial activity in only 20 mins. The observed increased resistance of this enzyme may be due to the unique supramolecular assembly of the enzyme's 12 subunits. Each subunit is aligned such that a compact spherical structure is formed with the active site of each subunit facing the interior space of the sphere. Pores positioned throughout the sphere provide urea access to the enzyme's active sites (Dunn and Grütter, *Nat. Struct. Biol.* 2001, 8; Ha et al., *Nat. Struct. Biol.* 2001, 8). Charged residues on the surface of the sphere may act as fluoride sinks, thereby, preventing fluoride from entering the sphere and interacting with the nickel ions in the active sites of the enzyme.



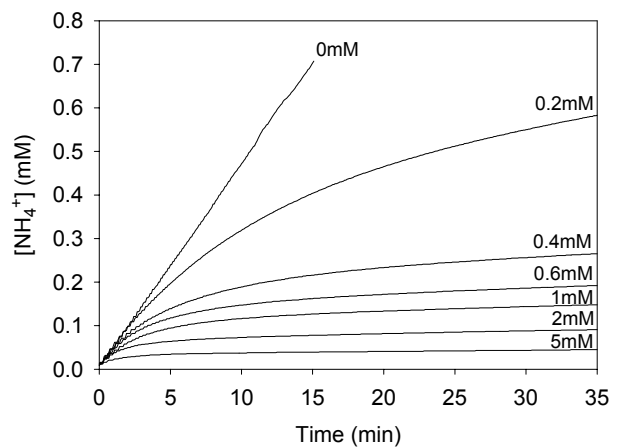
(A)



(B)



(C)



(D)

**Figure 7.** Inhibition of jack bean urease (A), *Helicobacter pylori* urease (B), stable jack bean urease supplied by Roche Molecular Biochemicals (C), and recombinant *Klebsiella aerogenes* (FRKAU 9-1) mutant urease (D) by fluoride. The concentration in millimolar of fluoride present in each assay is indicated.

*Improving resistance of biocatalytic buffers to fluoride inhibition*

Our preliminary results illustrating the degree to which ureases are inhibited by fluoride suggest that strategies of protecting the enzyme must be employed to prevent inactivation of the urease-based buffer.

One approach to limiting the impact of fluoride on urease activity that was investigated involved the addition of calcium to the system of reactions. Calcium present will complex with the free fluoride generated during nerve agent degradation resulting in the formation of an insoluble salt, which precipitates from the reaction (**Figure 8**).

Calcium treatment is commonly employed in industry for the purification of wastewater containing elevated fluoride levels.

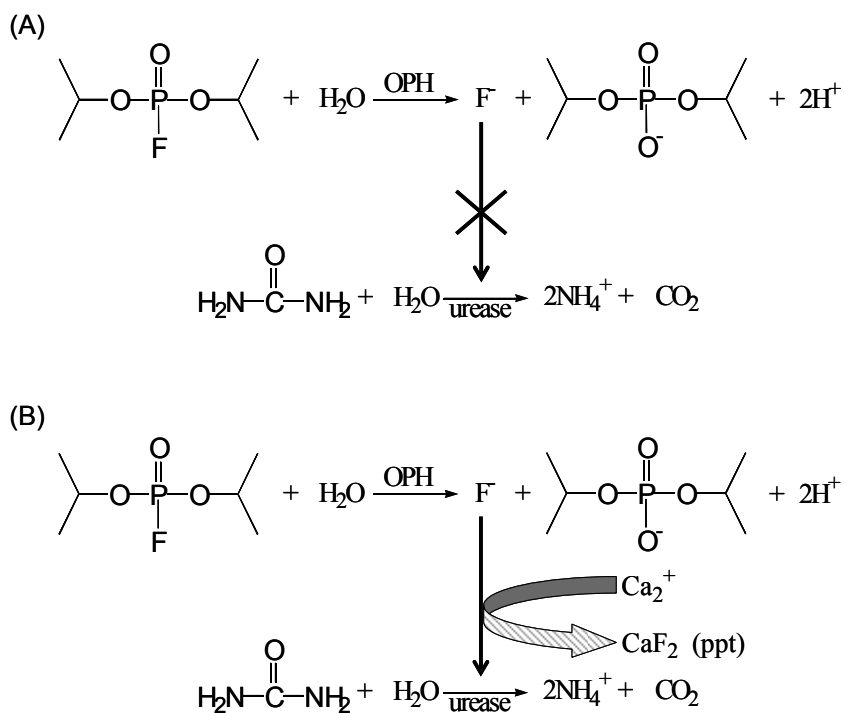


**Figure 8. Calcium-induced precipitation of fluoride for the protection of urease in biocatalytic pH control. (A) Fluoride generated from DFP hydrolysis will inhibit urease activity, thereby, destroying the buffering ability of the system. (B) The addition of calcium induces precipitation of fluoride, thus preventing fluoride inhibition of urease.**

Our preliminary results indicated that OPH and urease activities are largely unaffected by calcium up to 0.5 M (**Figure 9**). At higher calcium concentrations, the activity of both enzymes drops off considerably, presumably due to altering of the balance of electrostatic interactions within the enzyme structures. This ultimately brings to light the compromise between accommodating higher fluoride levels with increasing calcium concentrations and retaining enzyme activity.

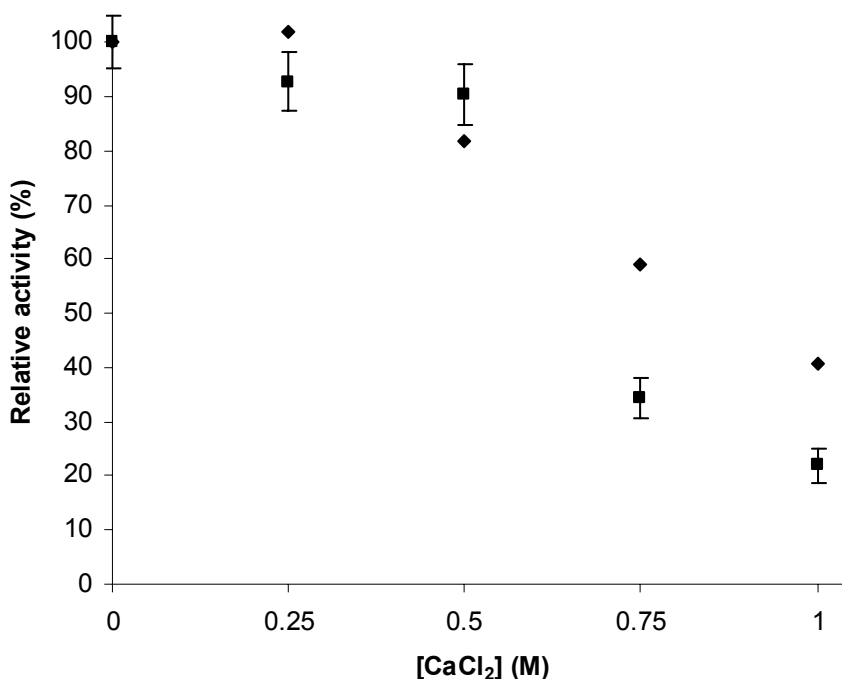


**Figure 9. The effect of calcium on the activity of jack bean urease (♦) and OPH (■).**

Model decontamination reactions (2 mM DFP, 250 mM urea, 0.2 units/mL OPH, 0.5 units/mL urease) in which urease-catalyzed urea hydrolysis was used to buffer the degradation of DFP by OPH were then performed with and without calcium. In the

absence of calcium, the conversion of DFP under the model conditions reached 99.9 % within 24 mins (**Figure 10**). The pH during decontamination was maintained between 7.2 and 7.5 until the conversion of DFP exceeded 85 % at which point the pH steadily increased. As described in the case for paraoxon hydrolysis, this observed increase in pH is due to the effect of substrate depletion on the degree of enzyme saturation. Eventually, the rate of DFP degradation becomes negligible relative to the rate of urea hydrolysis and the dynamic equilibrium is altered.

The model decontamination reaction was then performed in the same manner with 0.5 M calcium chloride. However, no improvement in the rate of DFP degradation was observed (**Figure 11**). The pH and DFP conversion profiles closely matched the corresponding profiles in the reaction without calcium.

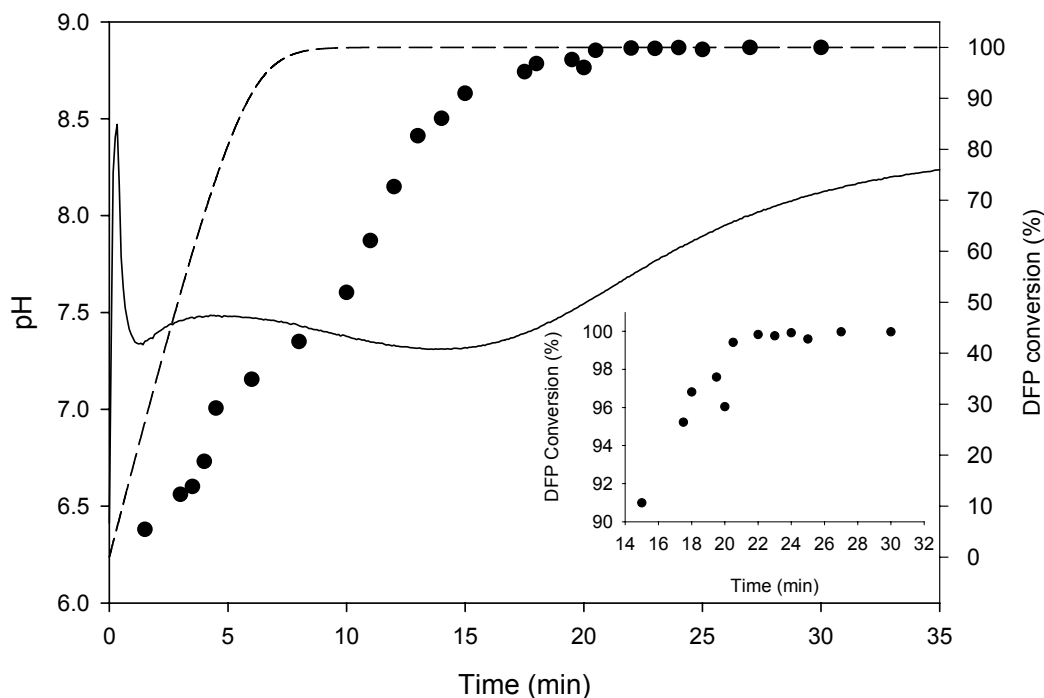


**Figure 10. Urease buffered detoxification of DFP. The solid line and closed circles represent the measured pH and DFP conversion profiles respectively. The dashed**

line represents the model generated DFP conversion profile. The data in the region of 100 % agent conversion is magnified (inset plot).

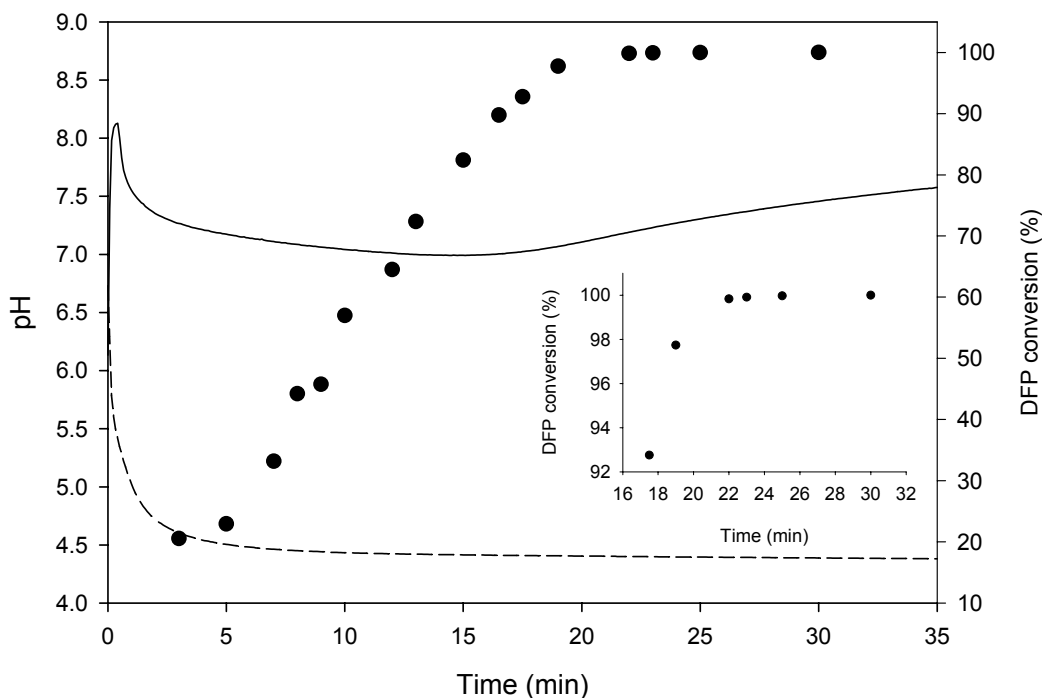


**Figure 11. Urease buffered detoxification of DFP in the presence of 500 mM calcium. The solid line and closed circles represent the measured pH and DFP conversion profiles respectively. The data in the region of 100 % agent conversion is magnified (inset plot). The dashed line corresponds to the pH profile of the reaction in the absence of urease. Based on the drop in pH, the conversion of DFP after 40 mins was calculated to be 1.1 %.**

These results confirm that, at the levels of enzyme activities used, the addition of calcium had no mitigating effect on the fluoride inhibition of urease and ultimately the rate of detoxification, which is essential in limiting the exposure of a chemical weapon. Presumably, when employing lower levels of enzyme activities, the impact of calcium on the rate of detoxification would have been more pronounced. That being said, calcium may have considerable utility in applications of urease buffers where it is critical that urease remain active over long periods of time such as in biosensors.

A second means of improving the ability to buffer the degradation of nerve agents containing a reactive P-F bond that was investigated involved the use of alternative base-producing enzymatic reactions. We screened the activity of a range of enzymes including adenosine deaminase (ADA) that catalyze the formation of base for fluoride sensitivity. ADA, which catalyzes the conversion of adenosine to inosine and ammonium, was identified as a candidate for use in biocatalytic pH control systems due to low fluoride sensitivity (**Figure 12**). The enzyme retains 23 % of its intrinsic activity when assayed in the presence of 200 mM fluoride (**Figure 13**).

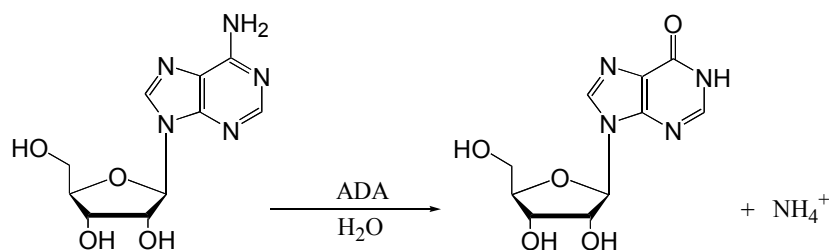


**Figure 12. ADA-catalyzed conversion of adenosine.**

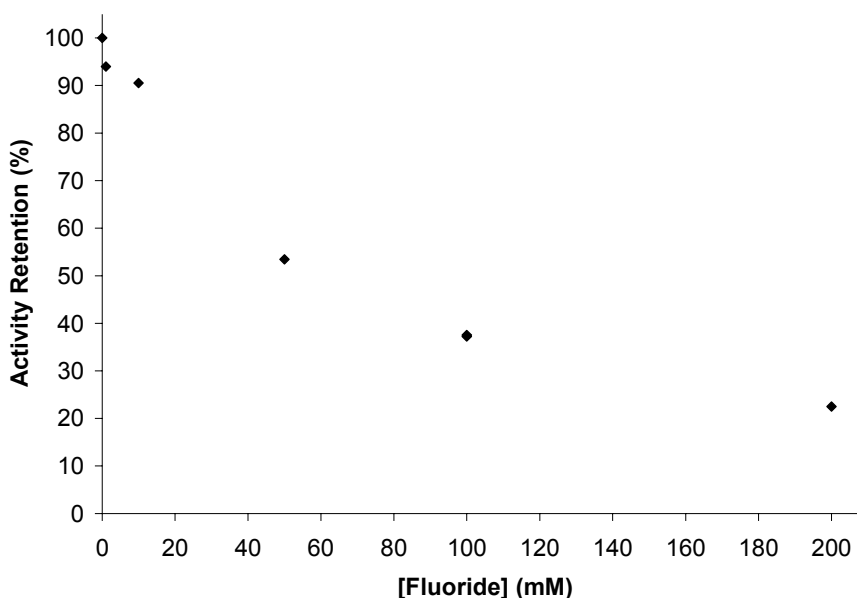


**Figure 13. The effect of fluoride on ADA activity. ADA was assayed using the pH-stat assay method.**

Decontamination experiments verified the ability to buffer the complete degradation of 5 mM aqueous DFP using ADA-catalyzed adenosine hydrolysis (**Figure 14**). The pH and DFP conversion profiles are similar to those observed in the decontamination reactions in which urease is employed. As shown in **Figure 13**, the amount of fluoride released from this level of agent does not significantly impact ADA activity.

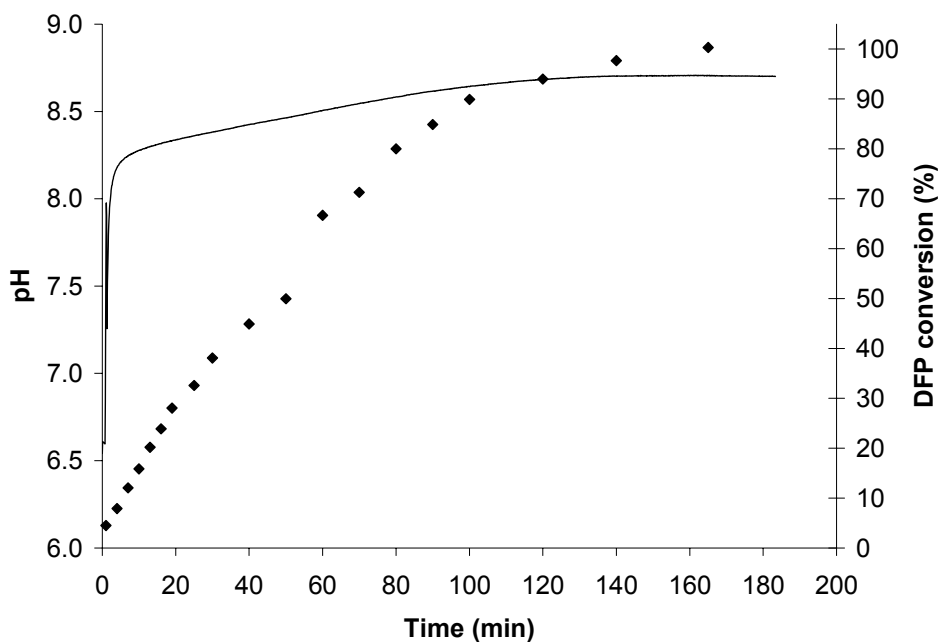


**Figure 14. Decontamination of DFP using ADA-catalyzed adenosine hydrolysis as the buffering agent. The solid line corresponds and the closed diamonds correspond to the measured pH and DFP conversion profiles respectively.**

ADA and adenosine may be either used exclusively or supplemented to urease-based biocatalytic buffers to overcome fluoride inhibition during the decontamination of a broad spectrum of nerve agents.

*Biocatalytic pH control in low-water environments*

Many nerve agents are only slightly soluble at best in aqueous solutions and consequently, low-water systems or mixed solvent systems are ideal detoxification mediums. Examples of such mediums include fire-fighting foams and reversed-phase microemulsions and nanoemulsions. A portion of our efforts was focused towards assessing the use of biocatalytic pH control in these types of mediums. Specifically, we strove to develop methods of measuring pH in low-water environments and to determine the impact of surfactants and organic solvents within such mediums on the activity of the enzymes employed in biocatalytic pH control.

Our initial work demonstrated that standard electrodes do not accurately measure pH of the water core of micelles in a model water-in-oil microemulsion comprised of 13 vol % Tween 85, 8 vol % isopropanol, and 10 vol % aqueous buffer. This is due to a lack of water that is required to bridge the sample and reference electrodes. An alternative means of monitoring pH we investigated involved the use of pH-sensitive dyes. We have shown that one such dye, phenol red, undergoes a color transition in the near neutral pH region when placed in the model reversed micelle solution (Figure 15). The  $pK_a$  of phenol red was approximately 1 pH unit in the reversed micelle solution relative to in buffer. The use of dyes as pH indicators served as a valuable tool for detecting variations in pH during hydrolytic enzyme assays and biocatalytic pH control experiments in low-water environments.

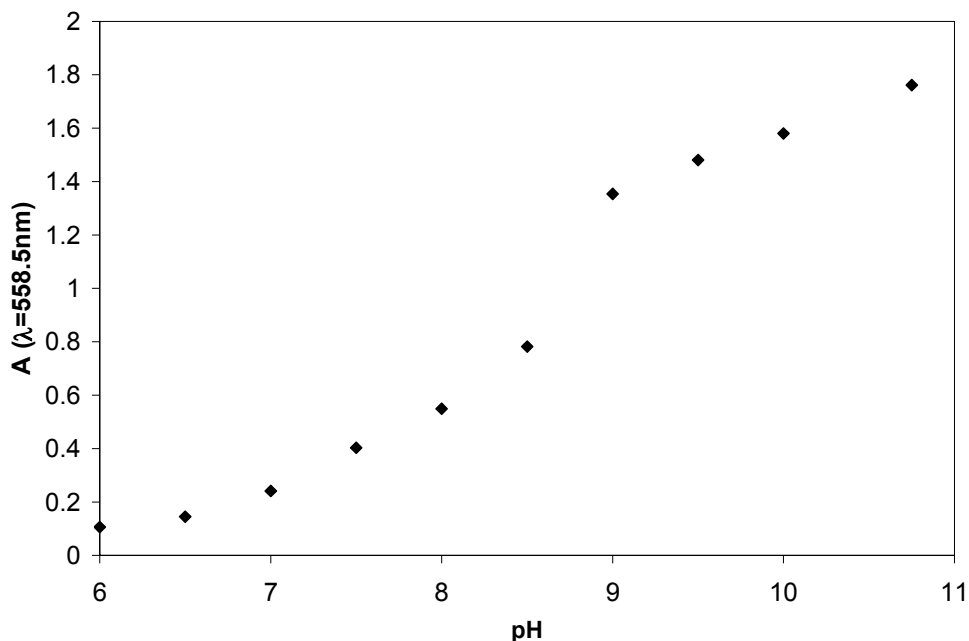


**Figure 15. Color transition of phenol red in reversed-micelle solution (13 vol % Tween 85, 8 vol % isopropanol, 10 vol % aqueous buffer). The pH of the buffer used in the preparation of the micelle solution is indicated on the x-axis.**

Earlier work from our lab has demonstrated that OPH, when placed in a water-ion-oil microemulsion, partitions to either the surfactant layer or the aqueous phase depending on the amount of water in the emulsion and effectively degrades paraoxon, parathion, and methyl-paraoxon (Komives et al., *Biotechnol. Bioeng.* 1993, 43).

However, little is known about the activity of ureases in such environments. We proceeded to assay the activity of jack bean urease in the model reversed micelle system previously described by using phenol red to measure the increase in pH resulting from the catalyzed urea hydrolysis. Our results indicate that, as is the case with OPH, urease is indeed active in this medium. However, stability studies show that urease is unstable in the microemulsion with the half-life ( $t_{1/2}$ ) of the enzyme being less than 20 mins (Figure

16). Efforts to stabilize urease in such mediums must be further investigated to make urease-based buffers a viable means of controlling pH in low-water decontaminants.

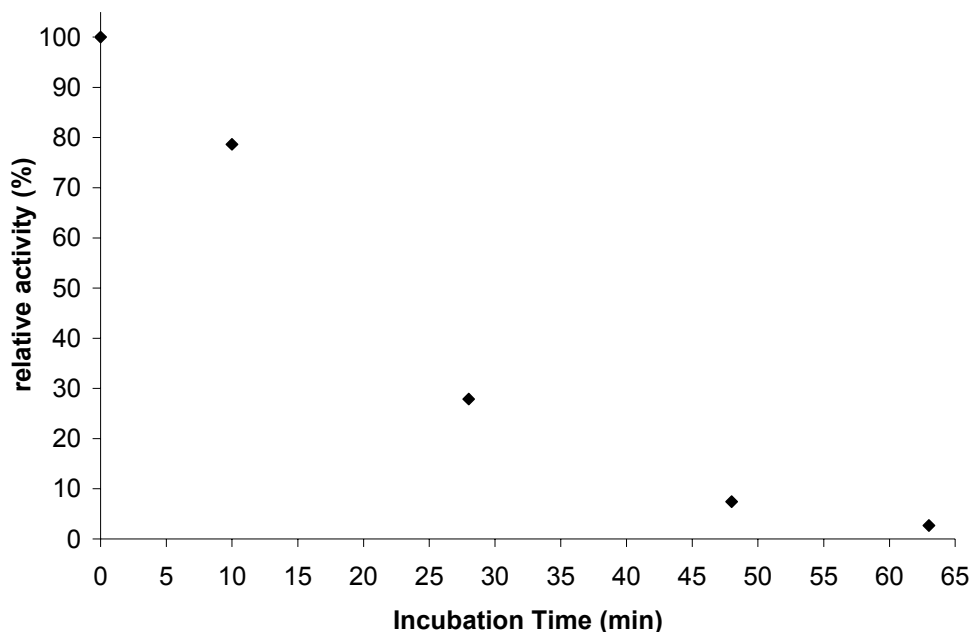


**Figure 16. Stability of urease in reversed micelle solution (13 vol % Tween 85, 8 vol % isopropanol, 10 vol % aqueous solution comprised of 50 mM sodium chloride, 0.15 mM cobalt chloride, and 7.8 units/mL jack bean urease at pH 6). The assay reaction was initiated by the addition of urea to a final concentration of 1 M. The increase in pH over time was recorded and used as a measure of urease activity.**

## Conclusions

Our results demonstrate that biocatalytic process can be employed to buffer the enzymatic degradation of nerve agents and that this approach to pH control overcomes many of the problems presented by conventional biological buffers. Specifically, paraoxon and DFP were degraded to completion using urease-catalyzed urea hydrolysis as the buffering agent. A theoretical model was constructed based on the pH-dependent activity profiles of the enzymes that successfully predicted the system pH and agent conversion over a range of OPH to urease ratios.

Additional results revealed that ureases from jack bean and *H. pylori* as well as the FRKAU 9-1 mutant urease from *K. aerogenes* were significantly inhibited by fluoride, a hydrolysis product of many G-type nerve agents. This inhibition will limit the amount of such agents that can be degraded when employing urease based buffers. As a means of improving the resistance of biocatalytic buffers to fluoride inhibition, we investigated the use of scavengers that induce precipitation of the inhibitor, namely calcium, and alternative base-producing enzymatic reactions. While calcium proved to be effective in precipitating free fluoride ions from solution, the addition of calcium to decontamination reactions did not mediate the inhibition of fluoride. Moreover, ADA activity was markedly less sensitive to fluoride than the activity of the ureases previously described and was successfully used to buffer the decontamination of aqueous DFP.

The research made possible by the funding of this project represents a significant contribution to the field of chemical weapons defense and biocatalytic detoxification in particular.

### **Summary of Papers Published or Presented**

Russell AJ, Erbeidiner M, DeFrank JJ, Kaar J, Drevon G. Catalytic buffers enable positive-response inhibition-based sensing of nerve agents. *Biotechnol Bioengr* 2002;77:352-357.

Russell AJ, Kaar JL, Berberich JA. Using biotechnology to detect and counteract chemical weapons. *The Bridge* (a publication of the National Academy of Engineering) 2003;33:19-24.

Kaar JL, Koepsel RR, DeFrank JJ, Russell AJ. Biocatalytic pH control for nerve agent detoxification. Presented at American Institute of Chemical Engineers Annual Meeting, Austin, TX 2004.

### **Technical Reports Submitted to ARO**

2002 Interim Progress Report (submitted March 2003)  
2003 Interim Progress Report (submitted March 2004)  
2004 Interim Progress Report (submitted July 2004)

**Scientific Personnel Supported by the Project**

Joel L. Kaar (Ph.D. graduate student) – University of Pittsburgh, Department of Chemical Engineering

Dr. Richard R. Koepsel (research professor) – University of Pittsburgh, Department of Chemical Engineering